**NUCLEAR DATA AND MEASUREMENTS SERIES**

**ANL/NDM-60**

# Gamma-Ray Detector Calibration Methods Utilized in the Argonne FNG Group Activation Cross Section Measurement Program

by

James W. Meadows and Donald L. Smith

June 1984

**ARGONNE NATIONAL LABORATORY,**
**ARGONNE, ILLINOIS 60439, U.S.A.**

# NUCLEAR DATA AND MEASUREMENTS SERIES

ANL/NDM-60

## GAMMA-RAY DETECTOR CALIBRATION METHODS UTILIZED IN THE ARGONNE FNG GROUP ACTIVATION CROSS SECTION MEASUREMENT PROGRAM

by

James W. Meadows and Donald L. Smith

June 1984

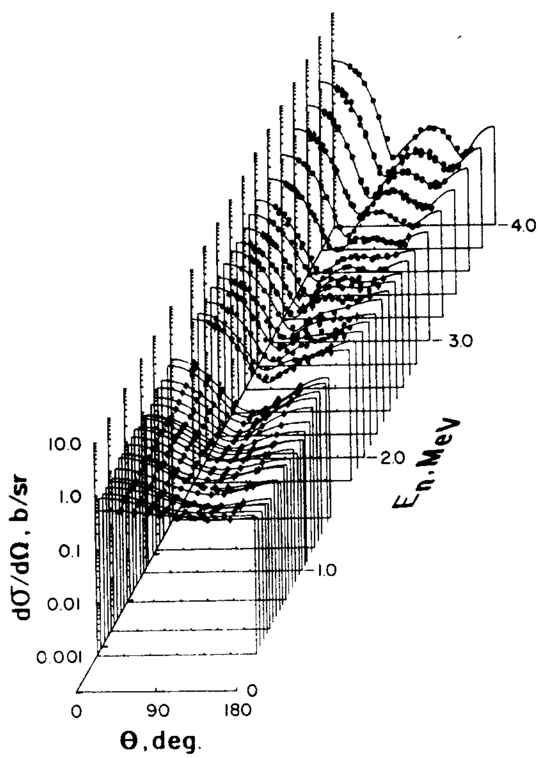


U of C - AUA - USDOE

ARGONNE NATIONAL LABORATORY,
ARGONNE, ILLINOIS 60439, U.S.A.

ANL/NDM-60

# GAMMA-RAY DETECTOR CALIBRATION METHODS UTILIZED IN THE ARGONNE FNG GROUP ACTIVATION CROSS SECTION MEASUREMENT PROGRAM

by

James W. Meadows and Donald L. Smith

June 1984

E

GAMMA-RAY DETECTOR CALIBRATION. Standard sources. $\gamma$-$\gamma$ coincidence counting. Angular correlations. $^{60}Co$ and $^{48}Sc$ decay. Error analysis.

*This work supported by the U. S. Department of Energy.

Applied Physics Division
Argonne National Laboratory
9700 South Cass Avenue
Argonne, Illinois 60439
U.S.A.

## NUCLEAR DATA AND MEASUREMENTS SERIES

The Nuclear Data and Measurements Series presents results of studies in the field of microscopic nuclear data. The primary objective is the dissemination of information in the comprehensive form required for nuclear technology applications. This Series is devoted to: a) measured microscopic nuclear parameters, b) experimental techniques and facilities employed in measurements, c) the analysis, correlation and interpretation of nuclear data, and d) the evaluation of nuclear data. Contributions to this Series are reviewed to assure technical competence and, unless otherwise stated, the contents can be formally referenced. This Series does not supplant formal journal publication but it does provide the more extensive information required for technological applications (e.g., tabulated numerical data) in a timely manner.

INFORMATION ABOUT OTHER ISSUES IN THE ANL/NDM SERIES:

A list of titles and authors for reports ANL/NDM-1 through ANL/NDM-50 can be obtained by referring to any report of this series numbered ANL/NDM-51 through ANL/NDM-76. Requests for a complete list of titles or for copies of previous reports should be directed to:

Section Secretary
Applied Nuclear Physics Section
Applied Physics Division
Building 316
Argonne National Laboratory
9700 South Cass Avenue
Argonne, Illinois 60439
USA

ANL/NDM-51 Measured and Evaluated Neutron Cross Sections of Elemental Bismuth by A. Smith, P. Guenther, D. Smith and J. Whalen, April 1980.

ANL/NDM-52 Neutron Total and Scattering Cross Sections of $^{6}Li$ in the Few MeV Region by P. Guenther, A. Smith and J. Whalen, February 1980.

ANL/NDM-53 Neutron Source Investigations in Support of the Cross Section Program at the Argonne Fast-Neutron Generator by James W. Meadows and Donald L. Smith, May 1980.

ANL/NDM-54 The Nonelastic-Scattering Cross Sections of Elemental Nickel by A. B. Smith, P. T. Guenther and J. F. Whalen, June 1980.

ANL/NDM-55 Thermal Neutron Calibration of a Tritium Extraction Facility using the $^{6}Li(n,t)^{4}He/^{197}Au(n,\gamma)^{198}Au$ Cross Section Ratio for Standardization by M. M. Bretscher and D. L. Smith, August 1980.

ANL/NDM-56 Fast-Neutron Interactions with $^{182}W$, $^{184}W$ and $^{186}W$ by P. T. Guenther, A. B. Smith and J. F. Whalen, December 1980.

ANL/NDM-57 The Total, Elastic- and Inelastic-Scattering Fast-Neutron Cross Sections of Natural Chromium by Peter T. Guenther, Alan B. Smith and James F. Whalen, January 1981.

ANL/NDM-58 Review of Measurement Techniques for the Neutron Capture Process by W. P. Poenitz, August 1981.

ANL/NDM-59 Review of the Importance of the Neutron Capture Process in Fission Reactors by Wolfgang P. Poenitz, July 1981.

ANL/NDM-60 Gamma-Ray Detector Calibration Methods Utilized in the Argonne FNG Group Activation Cross Section Measurement Program by James W. Meadows and Donald L. Smith, April 1984 [Present report-see notice at the end of this list]

ANL/NDM-61 Fast-neutron Total and Scattering Cross Sections of $^{58}$Ni by Carl Budtz-Jørgensen, Peter T. Guenther, Alan B. Smith and James F. Whalen, September 1981.

ANL/NDM-62 Covariance Matrices and Applications to the Field of Nuclear Data by Donald L. Smith, November 1981.

ANL/NDM-63 On Neutron Inelastic-Scattering Cross Sections of $^{232}$Th, $^{233}$U, $^{235}$U, $^{238}$U, $^{239}$U, and $^{239}$Pu and $^{240}$Pu by Alan B. Smith and Peter T. Guenther, January 1982.

ANL/NDM-64 The Fission-Fragment Angular Distributions and Total Kinetic Energies for $^{235}$U(n,f) from 0.18 to 8.83 MeV by James W. Meadows and Carl Budtz-Jørgensen, January 1982.

ANL/NDM-65 Note on the Elastic Scattering of Several-MeV Neutrons from Elemental Calcium by Alan B. Smith and Peter T. Guenther, March 1982.

ANL/NDM-66 Fast-neutron Scattering Cross Sections of Elemental Silver by Alan B. Smith and Peter T. Guenther, May 1982.

ANL/NDM-67 Non-evaluation Applications for Covariance Matrices by Donald L. Smith, July 1982.

ANL/NDM-68 Fast-neutron Total and Scattering Cross Sections of $^{103}$Rh by Alan B. Smith, Peter T. Guenther and James F. Whalen, July 1982.

ANL/NDM-69 Fast-neutron Scattering Cross Sections of Elemental Zirconium by Alan B. Smith and Peter T. Guenther, December 1982.

ANL/NDM-70 Fast-neutron Total and Scattering Cross Sections of Niobium by Alan B. Smith, Peter T. Guenther and James F. Whalen, July 1982.

ANL/NDM-71 Fast-neutron Total and Scattering Cross Sections of Elemental Palladium by Alan B. Smith, Peter T. Guenther and James F. Whalen, June 1982.

ANL/NDM-72 Fast-neutron Scattering from Elemental Cadmium by Alan B. Smith and Peter T. Guenther, July 1982.

ANL/NDM-73 Fast-neutron Elastic-Scattering Cross Sections of Elemental Tin by C. Budtz-Jørgensen, Peter T. Guenther and Alan B. Smith, July 1982.

ANL/NDM-74 Evaluation of the $^{238}$U Neutron Total Cross Section by Wolfgang Poenitz, Alan B. Smith and Robert Howerton, December 1982.

ANL/NDM-75 Neutron Total and Scattering Cross Sections of Elemental Antimony by Alan B. Smith, Peter T. Guenther and James F. Whalen, September 1982.

ANL/NDM-76 Scattering of Fast-Neutrons from Elemental Molybdenum by Alan B. Smith and Peter T. Guenther, November 1982.

ANL/NDM-77 A Least-Squares Method for Deriving Reaction Differential Cross Section Information from Measurements Performed in Diverse Neutron Fields by Donald L. Smith, November 1982.

ANL/NDM-78 Fast-Neutron Total and Elastic-Scattering Cross Sections of Elemental Indium by A. B. Smith, P. T. Guenther, and J. F. Whalen, November 1982.

ANL/NDM-79 Few-MeV Neutrons Incident on Yttrium by C. Budtz-Jørgensen, P. Guenther, A. Smith and J. Whalen, June 1983.

ANL/NDM-80 Neutron Total Cross Section Measurements in the Energy Region from 47 keV to 20 MeV by W. P. Poenitz and J. F. Whalen, July 1983.

ANL/NDM-81 Covariances for Neutron Cross Sections Calculated Using a Regional Model Based on Elemental-Model Fits to Experimental Data by Donald L. Smith and Peter T. Guenther, November 1983.

ANL/NDM-82 Reaction Differential Cross Sections from the Least-Squares Unfolding of Ratio Data Measured in Diverse Neutron Fields by D. L. Smith, January 1984.

ANL/NDM-83 The Fission Cross Sections of Some Thorium, Uranium, Neptunium and Plutonium Isotopes Relative to $^{235}$U by J. W. Meadows, October 1983.

ANL/NDM-84 $^{235}$U and $^{239}$Pu Sample-Mass Determinations and Intercomparisons by W. P. Poenitz and J. W. Meadows, November, 1983.

NOTICE: The present report has been assigned the number ANL/NDM-60 because another report originally intended for that slot was never completed and the title has therefore been withdrawn.

TABLE OF CONTENTS

# GAMMA-RAY DETECTOR CALIBRATION METHODS UTILIZED IN THE ARGONNE FNG GROUP ACTIVATION CROSS SECTION MEASUREMENT PROGRAM*

by

James W. Meadows and Donald L. Smith

Applied Physics Division
Argonne National Laboratory
Argonne, Illinois 60439
USA

ABSTRACT

The gamma-ray detector calibration methods utilized in the program of activation measurements at the ANL Fast Neutron Generator are described. The basic methods are gamma-gamma coincidence counting and comparison with calibrated sources. These methods are illustrated and compared using $^{60}Co$ and $^{48}Sc$ sources, and errors are discussed.

*This work supported by the U.S. Department of Energy.

# I. INTRODUCTION

Gamma counting is of considerable importance in nuclear science and, in a continuing program of activation measurements at the ANL Fast Neutron Generator, we have put together a set of procedures for such measurements. These have been referred to in several reports (e.g. ref. 1-3) by name and described as "standard" procedures. However the term "standard" is rather nebulous in this context, and the same general procedure performed by different experimentors can differ in many significant details.

This report describes in some detail our methods of determining absolute disintergration rates by gamma counting using high-resolution germanium detectors. The basic methods are (1) gamma-gamma coincidence counting using either one or two detectors and (2) comparison of unknown sources with calibrated sources. When possible these methods are used directly. In other cases they are used to construct suitable efficiency curves. The necessary sum-coincidence, sample-absorption and angular-correlation corrections are calculated by methods described in Section II. The results of measurements using both methods are compared in Section III. Finally, there is a brief discussion of the major sources of error.

# II. METHODS AND PROCEDURES

## A. Absolute Decay Rates by Gamma-Gamma Coincidence Counting

Coincidence counting is a powerful tool for the measurement of absolute decay rates of many radioactive isotopes since it is basically independent of the detector efficiences. This technique was early used for this purpose by Dunworth (4) who applied it to the almost ideal case of a beta transition followed by a gamma transition. The decay is observed by two detectors, one sensitive only to beta-rays and the other sensitive only to gamma-rays. If we ignore any background and accidental coincidences, the count rates for the individual detectors and the coincidence rate can be expressed as

$$R_\beta = \varepsilon_\beta \lambda N \qquad (1)$$

$$R_\gamma = \varepsilon_\gamma \lambda N \qquad (2)$$

$$R_{\beta\gamma} = \varepsilon_\gamma \varepsilon_\beta \lambda N \qquad (3)$$

where R is the count rate, $\varepsilon$ is the detector efficiency, N is the number of atoms of the radioactive isotope and $\lambda$ is the decay constant. Combining Eqs. (1), (2) and (3) gives the decay rate,

$$\lambda N = \frac{R_\beta R_\gamma}{R_{\beta\gamma}} \qquad (4)$$

In principal, the coincidence technique can be applied to any pair of transitions in a decay process, including gamma-gamma cascades, providing there are detectors that can separately detect each member of the pair. In practice the development of high-resolution germanium detectors has made gamma-gamma coincidence counting a very useful technique. Although these detectors are capable of completely separating the full-energy peaks, they cannot separate the Compton distributions, and they remain sensitive to all the gamma-rays emitted. This causes the phenomenon of sum-coincidence losses, but it also opens the possibility of doing coincidence counting with a single detector, where the coincidence rate is measured using the sum peak for the two gamma-rays involved.

Consider a general radioactive decay that proceeds by beta-emission, or other means, to serveral excited levels in the final nucleus. Each of these levels may decay by one or more paths. As a result, there are a number of possible gamma-rays, some in coincidence, some not, and some partially in coincidence. However, the decay scheme can be split into several independent parallel cascades that do not branch. A simple case is illustrated in Fig. 1 which shows the principal gamma-ray decay paths (5) of $^{48}$Sc. For a single cascade, the count rate for the full-energy peak of $\gamma_i$ is the probability of detecting $\gamma_i$ times the probability of not detecting any other gamma in that cascade. The total full-energy peak count rate in detector "a" is given by the sum over all cascades, $\ell$, that contain $\gamma_i$:

$$R_i^a = \lambda N e_i^a \sum_\ell w_\ell \prod_{k \neq i} (1-\varepsilon_k^a F_{ik}^{aa}) = \lambda N e_i^a S_i^a \qquad (5)$$

$e_i^a$ = the full energy peak efficiency for $\gamma_i$ in detector "a",

$F_{ik}^{aa}$ = the angular correlation coefficient for $\gamma$'s i and k in detector "a",

$\varepsilon_k^a$ = the total efficiency of detector "a" for $\gamma_k$,

$w_\ell$ = the probability of the decay proceeding by cascade $\ell$.

There are similar expressions for the other $\gamma$'s and detectors.

If only one detector is used the coincidence rate may be obtained from the area under the sum peak for $\gamma_i$ and $\gamma_j$.

$$\begin{aligned} R_{ij}^{aa} &= \lambda N e_i^a e_j^a F_{ij}^{aa} \sum_\ell w_\ell \prod_{k \neq i,j} (1-\varepsilon_k^a\, F_{ik}^{aa}) \\ &= \lambda N e_i^a e_k^a F_{ij}^{aa} S_{ij}^{aa} \end{aligned} \qquad (6)$$

The sum over $\ell$ includes all those cascades that include both $\gamma_i$ and $\gamma_j$. The decay rate can be obtained form the measured decay rates by

$$\lambda N = \frac{\bar{R}_i^a \bar{R}_j^a F_{ij}^{aa} S_{ij}^{aa}}{\bar{R}_{ij}^{aa} S_i^a S_j^a} \tag{7}$$

where $\bar{R}$ refers to measured quantities. There is no dependence on the full energy peak efficiencies, but the total efficiencies are needed to determine the sum-coincidence corrections, S. The experimental arrangement can be chosen so $\varepsilon \ll 1$ and the S approach 1. However, the coincidence rate will then be very low.

When two detectors are used, greater flexibility is obtained and the arrangement can be adapted to a specific problem. However, the experimental set-up is more complex and the sum coincidence corrections may depend on the specific arrangement used. A common technique is to use a full-energy peak from one detector to gate a second detector. This can give decay rates and also assist in the analysis of complicated spectra. In the present measurements we are primarily interested in measuring decay rates of samples that often have low activities, so the principal attraction of the two-detector arrangement is the possibility of increased coincidence rates. If the two detectors are of similar size, and the second one is located at about the same distance from the sample, the total coincidence rate will be increased by a factor of ~ 4.

An experimental arrangement that we often use is illustrated in Fig. 2. As in the single detector case, the coincidence events are identified by the sum peaks. The total coincidence rate can be considered as the sum of the four independent coincidence possibilities, and the amplifier gains can usually be adjusted so that the four sum peaks are seperated. However, this is not necessary so the zero levels and amplitudes can be carefully matched and only a single peak is observed. With complicated spectra, it may be necessary to set the single-channel analyser (SCA) windows to eliminate some of the coincidences, and thus simplify the sum-coincidence spectrum. This may introduce an additional complication since the coincidence rate, measured at the output of the summing amplifier, must be corrected for sum-coincidence losses that occur in that amplifier as well as for losses that occur within the individual detectors.

Measurements made with the SCA windows completely open (or removed) have the maximum coincidence rate and no problems with the $\varepsilon$. The singles rates are measured before entering the summing amplifier, and the sum-coincidence correction is given by Eq. (5). The total coincidence rate, $R_{ij}$, is

$$R_{ij} = R_{ij}^{aa} + R_{ij}^{bb} + R_{ij}^{ab} + R_{ij}^{ab} \quad . \tag{8}$$

Each term may be expressed as the product of the probabilities of detecting $\gamma_i$ and $\gamma_j$ in the indicated detectors, and the probability of not detecting any other $\gamma$ in the cascade in either detector. The general form is

$$\begin{aligned} R_{ij}^{ab} &= \lambda N e_i^a e_j^b F_{ij}^{ab} \sum w_\ell \prod_{k\neq i,j} (1-\varepsilon_k^a F_{ik}^{aa} - \varepsilon_k^b F_{ik}^{ab}) \\ &= \lambda N e_i^a e_j^b F_{ij}^{ab} S_{ij}^{ab} \quad . \end{aligned} \tag{9}$$

The decay rate based on the data obtained with this particular arrangement is

$$\begin{aligned} \lambda N = \Bigg[ & \frac{\bar{R}_i^a \bar{R}_j^a F_{ij}^{aa} S_{ij}^{aa}}{S_i^a S_j^a} + \frac{\bar{R}_i^b \bar{R}_j^b F_{ij}^{bb} S_{ij}^{bb}}{S_i^b S_j^b} \\ & + \frac{\bar{R}_i^a \bar{R}_j^b F_{ij}^{ab} S_{ij}^{ab}}{S_i^a S_j^b} + \frac{\bar{R}_i^b \bar{R}_j^a F_{ij}^{ba} S_{ij}^{ba}}{S_i^b S_j^a} \Bigg] \frac{1}{\bar{R}_{ij}} \quad . \end{aligned} \tag{10}$$

If $\gamma_i$ and $\gamma_j$ are detected in the same detector then part of the coincidence sum loss occurs in the sum amplifier and will depend on the SCA window settings. If the upper levels of the SCA windows are reduced so as to eliminate $R_{ij}^{aa}$ and $R_{ij}^{bb}$, then all the coincidence events will involve both detectors and all sum coincidence losses will occur within one or the other of the detectors. The decay rate will then be given by eq. (10) with the first two terms in the brackets deleted. If the SCA window widths are reduced so that side "a" accepts only the full energy peak of $\gamma_i$ and side "b" accepts into the full energy peak of $\gamma_j$ then only the third term will remain.

## B. Absolute Decay Rates by Comparison with Calibrated Gamma-ray Sources.

The calibrated sources are selected so there are several full-energy-peaks in the region of interest. These are essentially point sources and are mounted in holders that have negligible absorption. They are counted at a well-determined position in the range of 20 to 30 cm from the detector. At this distance, sum coincidence correction factors are very near 1 and may usually be neglected. The unknown samples are typically disks 25.4 mm in diameter and ~ 0.2 to ~ 7 mm thick. One or two of these are made sufficiently active to provide reasonable counting rates at the 20 to 30 cm distance. They are located so the centers of the samples correspond to the position of the calibrated sources, and their full-energy-peak count rates are measured. The full-energy-peak rates for the calibarated sources are then corrected to what they would be if the source material had been distributed uniformaly through a sample disk. These provide points for an efficiency curve which is fitted by

$$\log(e) = a+b\log(E_\gamma)+c(\log(E\gamma))^2 + \ldots \quad (11)$$

If $E_\gamma$ > 400 keV, and spans no more than ~ 400 keV, the linear form is usually sufficient. For wider ranges and lower energies additional terms may be required.

The above curve provides efficiencies for the full energy peaks of the gamma-rays from the samples and the decay rate is

$$\lambda N = \frac{R_i(d)}{I_i e_i(d)} \quad (12)$$

where $R_i$ is the full energy peak count rate for $\gamma_i$, $I_i$ is the number of $\gamma_i$ per decay and $e_i$ is the full energy peak efficiency at distance d. These samples are now used to determine the effective efficiencies at some closer position where like samples of lower activity can be conveniently counted. This procedure has the advantage of eliminating the need for sum-coincidence corrections, and systematic errors in determing the areas under the full-energy peaks tend to cancel.

In many cases it is not possible to produce enough activity in the sample for accurate counting at the 20-30 cm distance. Then, other reactions that produce radioactive products at higher activity levels are used to construct an efficiency curve at the close position. These samples may be of different sizes and materials. The required size and absorption corrections are then calculated using the procedures outlined below. Sum-coincidence correction factors are calculated according to Eq. (5).

## C. The Determination of Peak Areas

The type of measurements with which we are concerned involve pure samples, neutron beams of fairly low intensities and backgrounds that are fairly low and stable, so the resulting gamma-ray spectra are not complicated. Cases with more than three or four radioactive species present in significant amounts are quite rare, and most of the full-energy peaks are isolated. Peak areas are determined by substracting the underlying background components of the spectra; peak fitting techniques are avoided if possible. To determine the area under a peak, a window is set over it that is wide enough to include any tailing that occurs. Lesser windows are set above and below the peak window, and they are used to estimate the background which is approximated by a polynominal. A linear function is most often used, but if inspection of the spectra suggests that the underlying background has curvature, higher order terms may be included.

## D. The Calculation of the Total Efficiency ($\varepsilon$) and the Angular Correlation Factor (F).

In the analysis of coincidence results it is necessary to know the total efficiency ($\varepsilon$) and the angular correlation factor (F) for the gamma-rays involved. These quantities are very significant, and both depend on the sample-detector geometry. Table I gives some typical values of $\varepsilon$ and F for our usual counting arrangements. Increasing the sample-detector distance reduces the importance of $\varepsilon$, but it also reduces the coincidence rate and increases the importance of F. Since (monoenergetic) neutron activation measurements are often troubled by low count rates, this may make coincidence counting impractical. We have chosen to do most of the gamma counting in very poor geometry, and to calculate the necessary corrections.

We currently use the computer program GACON for this purpose. This program was designed to calculate sample absorption corrections for the full energy peaks, angular correlation coefficients, and efficient ratios for point an distributed sources. It was not designed to give true values of $\varepsilon$, but experience has shown that a fairly reliable values may be obtained if certain conditions are met.

The program uses the Monte Carlo method, and the sample-detector arrangement is shown in Fig. 3. Pairs of gamma-rays are assumed to originate uniformaly throughout the sample volume. The first gamma-ray direction is isotropic. The relative angle of the second gamma-ray, $\theta_{12}$, is weighted according to the angular correlation function. It is required that $\gamma_1$, be detected by detector-1 and $\gamma_2$ by detector-2. If the direction vector does not intersect the apropriate detector, the history is not followed. An interaction in the sample, absorber or detector core that sigificantly reduces the gamma-ray energy also terminates the history. The program input includes the dimensions indicated in Fig. 3, the gamma-ray cross sections and the coefficients of the angular correlation function. The program output yields the angular correlation factor, the sample and absorber factors and a "total" efficiency that is a little smaller than the true one.

However, it is possible to obtain a good approximation of the true total efficiency. $\varepsilon$ does not change rapidly with $E_\gamma$. Between 0.2 and 1.0 MeV the change is less than a factor of 2. Furthermore, the angular distribution of Compton-scattered gamma-rays is strongly peaked forward so the in/out scattering correction is small. Thus, only photo-electric interactions in the sample and absorber effect the total efficiency to any great extent. Gamma-rays that first interact in the inactive core region of a Ge(Li) detector will not contribute to the full-energy peak, but they usually produce some kind of signal and contribute to the total efficiency. If only photoelectric cross sections are entered for the sample and absorber, and if the diameter of the core region is set equal to zero, the efficiency calculated by GACON provides a good approximation for the true total efficiency, providing that the core region is not too large and that the sample and absorber are not too thick. For the examples presented in this report, the core occupies about 3% of the total detector volume and the gamma-ray transmission factor for the sample is $> 0.8$.

Some representative values of $\varepsilon$ and F are given in Table I.

## E. The Angular Correlation Function.

We are concerned with the angular correlation between two gamma-rays emitted by the same nucleus in a time interval that is short compared with the nuclear relaxation time. The analysis of this problem is based upon well-known methods from quantum mechanics involving angular momentum coupling rules. The expressions for the coefficients in gamma-gamma correlation functions can be quite complex, and they depend on the level spins involved, multipolarities and mixing ratios for the photon transitions, and on whether there are intermediate unobserved gamma-transitions. Segre (6) has provided a useful introductory discussion of this topic based, in part, on the 1953 review paper of Biedenharn and Rose (7). A report by Ferentz and Rosenzweig (8) includes some very extensive and useful tables. The monograph by Ferguson (9) also provides a useful general exposition of this topic, although the notation is somewhat different. Here we only present the results for the specific cases necessary for this report.

First, consider the sequential cascade of two gamma-rays, each with a well-defined multipolarity. An unpolarized nucleus in state $j_1$ decays to state j by emitting radiation of multipole order $L_1$. State j immediately decays to state $j_2$ by emitting radiation of multipole order $L_2$. Following Ref. 7, the angular correlation function in terms of Legendare polynominals is

$$\omega(\theta_{12}) = \sum_k F_k(L_1 j_1 j) F_k(L_2 j_2 j) P_k(\cos\theta). \quad (13)$$

where the sum is over terms limited by

$$0 \leq \text{even } k \leq \min\,(2j, 2L_i, 2L_2) \quad . \quad (14)$$

The F-coefficients are tabulated in Refs. 7 and 8. In terms of the more fundamental Clebsch-Gordon (C) and Racah (W) coefficients we can express the F-coefficient as

$$F_k(Lj_1j) = (-)^{j_1-j-1}(2j+1)^{1/2}(2L+1)C(LLk;1-1)W(jjLL;kj_1), \quad (15)$$

and thereby calculate values out of range of the tables if needed. The F-coefficient is defined so that

$$F_o(Lj_1j) = 1. \quad (16)$$

Thus Eq. 13 is normalized.

Consider now the case of the correlation between two gamma-rays when there is an intermediate, but unobserved, gamma-ray. An unpolarized nucleus in state $j_o$ decays through states $j_1$ and $j_2$ to state $j_3$ by emitting gamma-rays of multipolarity $L_o$, $L_1$ and $L_2$. The correlation function for the first and third gamma-rays is

$$\omega(\theta_{13}) = N \sum_k F_k\,(L_o j_o j_1)\; F_k\,(L_2 j_3 j_2)\; \delta(j_1 j_1 j_2 j_2;kL_1)\; P_k(\cos\,\theta), \quad (17)$$

where N is a normalization factor and is given by

$$N = (-)^{L_1-j_1-j_2}\left[(2j_1+1)(2j_2+1)\right]^{1/2} \quad , \tag{18}$$

and the sum is over terms limited by

$$o \leq k \leq \min(2L_o, 2L_2, 2j_1, 2j_2) \ . \tag{19}$$

The F are defined by Eq. 15 and the W are the Racah coefficients.

In this report we demonstrate our calibration methods by considering $^{48}Sc$ and $^{60}Co$ decay. The principal decay path in $^{48}Sc$ involves E2 transitions (see Fig. 1) representing a 6(2)4(2)2(2)0 cascade. The $^{60}Co$ cascade is similar but starts at 4.

The correlation function for pairs of successive gamma-rays is

$$\omega(\theta_{12}) = 1+0.1020P_2(\cos\theta)+0.00907P_4(\cos\theta) \tag{20}$$

For the case of an intermediate but unobserved gamma-ray the function is

$$\omega(\theta_{13}) = 1+0.1020P_2(\cos\theta)-0.0141P_4(\cos\theta) \tag{21}$$

## III. RESULTS

The methods described above were tested using the following $^{60}Co$ and $^{48}Sc$ samples:

M1 A 2.54-cm dia. × 0.57-cm thick cobalt disk weighing 24.1 g. The $^{60}Co$ activity was distributed unformaly through the volume of the disk.

M2 A thin, ~ 1 cm dia. deposit centered on a 025 mm thick stainless steel disk and sealed with a polyester film.

V-44 A 2.54-cm dia × 0.32-cm thick vanadium disk. The $^{48}Sc$ activity was produced by the $^{51}V(n,alpha)^{48}Sc$ reaction. This sample was reactivated during the course of these measurements and the corresponding activations are designated A, B and C.

Their decay rates were measured by comparing them to the three calibrated sources listed below:

| | |
|---|---|
| NBS SRM 4210-3 | A rather old (14 y) U.S. National Bureau of Standards $^{60}Co$ source mounted on a polyester film. |
| NBS SRM 4275-140 | A U.S. National bureau of Standards mixed source ($^{125}Sb$, $^{154}Eu$ and $^{155}Eu$) mounted on a polyester film. |
| LMRI EGAM-3 5243 | An $^{152}Eu$ source obtained from Laboratoire de Metrologie des Rayonnements Ionisants, Saclay, France. |

The decay rates of M1, M2 and V-44 were also measured by coincidence counting for a variety of detector-sample arrangements using both one and two detectors. The sum coincidence terms were calculated using the gamma-ray cross sections of Storm and Israel (10).

The results of the two methods and their intercomparison are shown in Table II. The agreement is consistent and fairly good. The decay rate obtained by coincidence counting does appear to be a little less than the standards comparison method, but the difference is well within the experimental error.

## IV. SOURCES OF ERROR

The principal sources of error are described below, and ranges of their magnitudes are given. The first three apply to the comparison with calibrated sources.

(1) Statistical. (0.6-1.1%) This is largely determined by the number of counts in the peaks but is also includes the error in the background substraction.

(2) Calibrated Sources. (0.6-0.7%) The error in the decay rates of these sources. It is assumed that there is no correlation among the three sources. The larger value applies to the measurements with the V-44 sample, where NBS 4210-3 was not used.

(3) Calibration Curve. (~ 1%) the error in the efficiencies based on the fit of Eq. (11) to the calibration measurements. The correlation among the different calibration curves is assumed to be zero.

The remaining errors apply to the coincidence measurements.

(4) Statistical. (0.5-2.5%) This is the same as (1) above. The range of error is given for $R_iR_j/R_{ij}$.

(5) Total Efficiencies. (0.2-1.6%) The range of error is for the decay rate. The error in $\varepsilon$ is ~ 5% and is largely due to the error in the gamma-ray cross sections (10).

(6) Background Subtraction. (~ 1%) This is an additional uncertainity due to the choice of the background windows and background function. We assume a 50% correlation.

We used a least-squares method for weighted averaging described in Section XI of Ref. 11, and calculated averages for all the avaliable ratios of activities deduced by the calibrated source comparison method relative to the coincidence counting method. These values appear in Table II along with corresponding normalized $\chi^2$ values. Some of these normalized $\chi^2$ values exceed unity by noticeable amounts, indicating that we may have underestimated some of the above errors or that there may be additional ones which we have not identified. Nevertheless, we had no rational basis for altering our original choices for the known partial errors and thus chose not to do so.

## V. SUMMARY

The various calibration methods discussed in this report seem suitable for dealing with most of the gamma-ray counting problems routinely encountered in our activation measurements program. The present investigation for $^{60}$Co and $^{48}$Sc activities indicated that we can expect to obtain agreement to within $\lesssim$ 2% between the two basic methods, comparisons with calibrated sources and coincidence counting, with a probable uncertainty of $\lesssim$ 2%, even for the relative poor-counting-geometry configurations we must often employ to measure weak activities. This level of accuracy is adequate for most of our program needs.

## REFERENCES


1. D. L. Smith and J. W. Meadows, Nucl. Sci. Eng. 58, 314(1975).
2. D. L. Smith and J. W. Meadows, Nucl. Sci. Eng. 76, 611(1980).
3. D. L. Smith and J. W. Meadows, Nucl. Sci. Eng. 81, 525(1982).
4. J. B. Dunsworth, Rev. Sci. Instr. 11, 167(1940).
5. Nuclear Level Schemes A=45 Through A=257 from Nuclear Data Sheets,
6. E. Segre, Experimental Nuclear Physics, Vol. III, p. 380, John Wiley & Sons, Inc., New York (1959).
7. L. C. Biedenharn and M. E. Rose, Rev. Mod, Phys. 25, 729(1953).
8. M. Ferentz and N. Rosenzweig, "Table of F Coefficients," ANL-5324, Argonne National Laboratory (1955).
9. A. J. Ferguson, Angular Correlation Methods in Gamma-Ray Spectroscopy, Interscience, New York (1965).
10. E. Storm and H. I. Israel, Nuclear Data Tables A7, 565 (1970).
11. Donald L. Smith, "Covariance Matrices and Applications to the Field of Nuclear Data," ANL/NDM-62, Argonne National Laboratory (1981).

Table 1. Representative Total Efficiencies and Angular Correlations Factors for the Single Detector Coincidence Measurement of $^{60}Co$ Sample M1[a].

| Distance[b] Cm | $\varepsilon_1$ | $\varepsilon_2$ | $F_{12}$ |
|---|---|---|---|
| 0.95 | 0.126 | 0.121 | 1.043 |
| 1.98 | 0.069 | 0.066 | 1.068 |
| 2.86 | 0.0455 | 0.0444 | 1.085 |
| 5.40 | 0.0194 | 0.0175 | 0.107 |

[a]Detector dimensions were 4.50 cm dia × 6.46 cm thick. Sample dimensions were 2.54 cm dia × 0.57 cm thick.

[b]Distance from center of sample to the front face of the detector.

Table II. The Results of Activity Measurements by Coincidence Counting and by Comparison with Standard Sources.

| Sample No. | Detector Distance A (cm) | Detector Distance B (cm) | Detector Angle (deg.) | Coincidence Count Rate | Coincidence Count Total Err (%) | Std. Comparison Rate | Std. Comparison Total Err (%) | Ratio | Total Err % |
|---|---|---|---|---|---|---|---|---|---|
| M1 | 0.95 | NA | 0 | 5453 | 1.96 | 5621 | 1.43 | 1.031 | 2.43 |
| | 1.98 | NA | 0 | 5446 | 1.58 | | | 1.032 | 2.13 |
| | 2.91 | NA | 0 | 5482 | 1.26 | | | 1.025 | 1.90 |
| | 5.40 | NA | 0 | 5835 | 2.54 | | | 0.963 | 2.92 |
| | | | | | | | average = | 1.020[a] | 1.82[a] |
| | | | | | | | $\chi^2$ = | 2.17 | |
| M2 | 0.97 | NA | 0 | 7462 | 2.98 | 7801 | 1.45 | 1.045 | 3.32 |
| | 2.61 | NA | 0 | 7924 | 1.87 | | | 0.984 | 2.36 |
| | 5.14 | NA | 0 | 7634 | 2.54 | | | 1.022 | 2.92 |
| | | | | | | | average = | 1.004[a] | 2.12[a] |
| | | | | | | | $\chi^2$ = | 2.43 | |
| M2 | 0.66 | 0.88 | 180 | 7710 | 1.78 | 7801 | 1.45 | 1.012 | 2.30 |
| | 1.45 | 1.93 | 180 | 7425 | 2.03 | | | 1.051 | 2.50 |
| | 0.81 | 3.52 | 180 | 7677 | 1.38 | | | 1.016 | 2.00 |
| | 6.21 | 5.18 | 90 | 7684 | 1.38 | | | 1.015 | 2.00 |
| | | | | | | | average = | 1.018[a] | 1.86[a] |
| | | | | | | | $\chi^2$ = | 1.59 | |
| V-44A | 0.95 | NA | 0 | 1136 | 1.79 | 1150 | 1.46 | 1.012 | 2.31 |
| V-44B | 0.95 | NA | 0 | 1311 | 2.11 | 1296 | 1.44 | 0.987 | 2.55 |
| V-44C | 0.95 | NA | 0 | 1289 | 2.12 | 1292 | 1.47 | 1.004 | 2.57 |
| | | | | | | | average = | 1.002 | 1.82 |
| | | | | | | | $\chi^2$ = | 0.41 | |
| | | | | | | | Grand Average = | 1.007 | 1.34 |
| | | | | | | | $\chi^2$ | 1.46 | |

[a]Weighted averages were calculated using a method described in Ref. 11 which takes all error sources and their correlations into consideration.

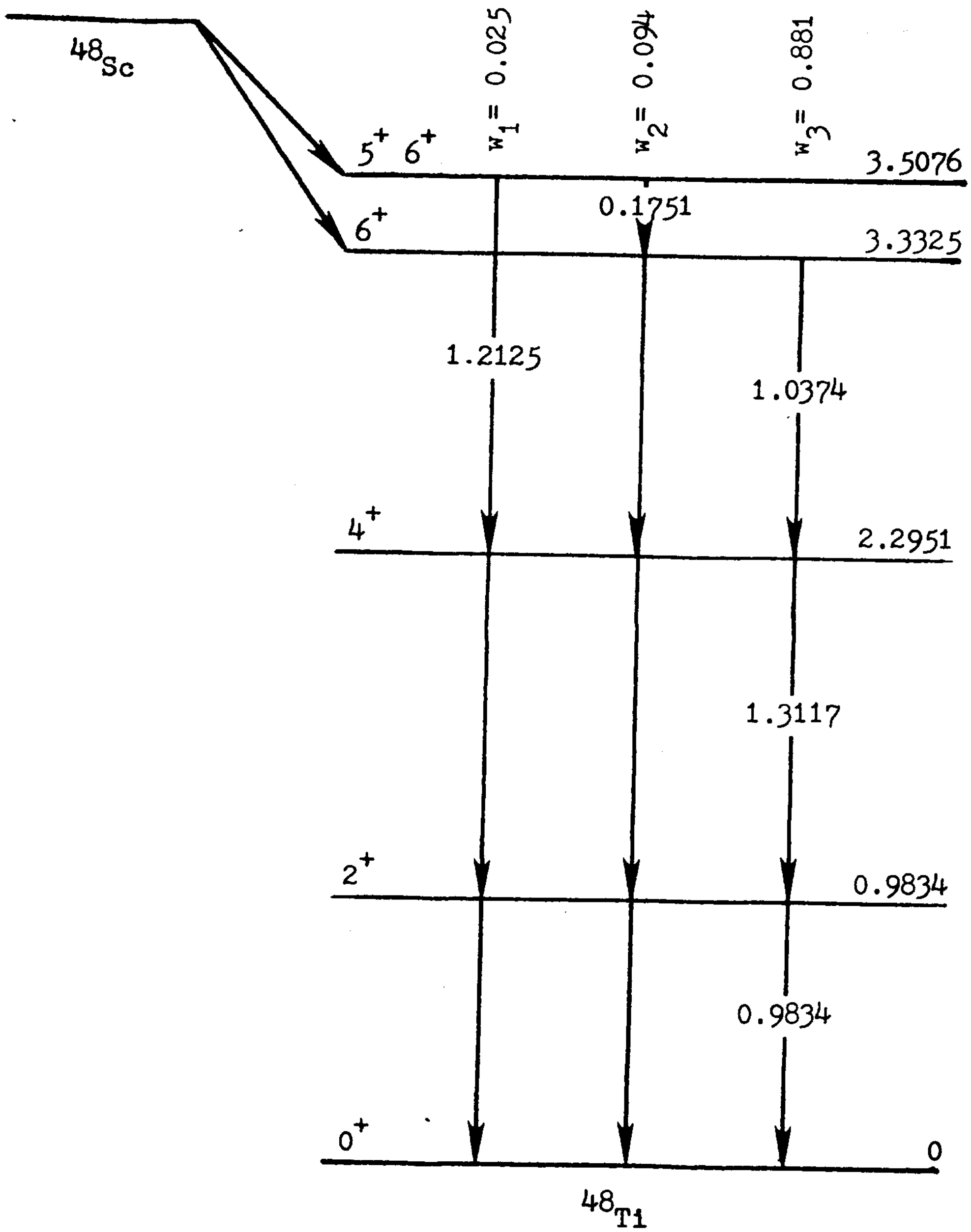


Fig. 1. The principal decay paths of $^{48}Sc$.

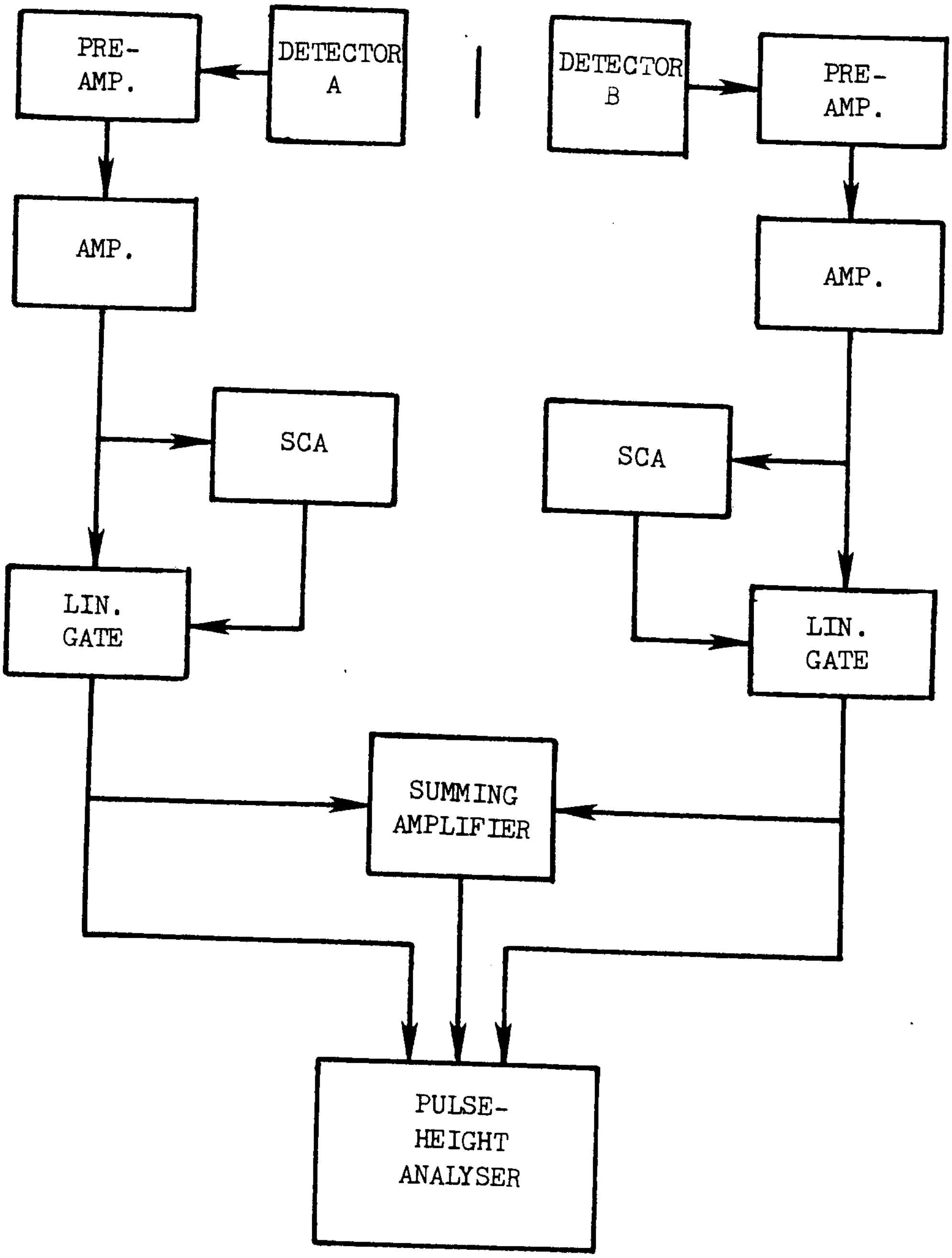


Fig. 2. A block diagram of a gamma-gamma coincidence arrangement.

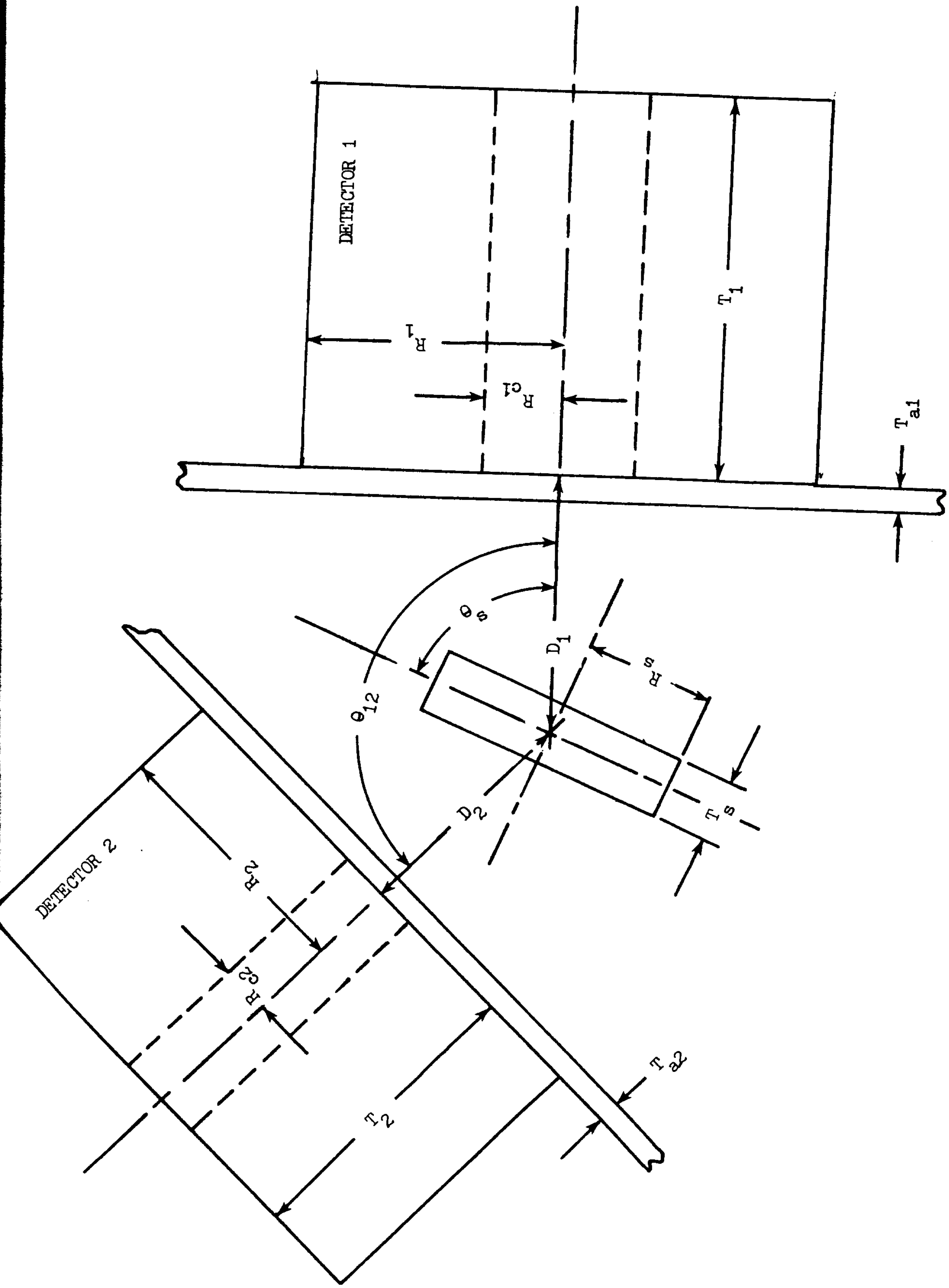


Fig. 3. The sample-detector arrangement for GACON calculations.